Cross-Node Humanoid Robot Control: FSM, PID, State-Space and LLM Integration

Shinichi Samizo, *Member, IEEE*

***Abstract*—This paper presents a proof-of-concept humanoid robot control framework that integrates finite-state machines (FSM), proportional–integral–derivative (PID) control, state-space methods (LQR/LQG), and large language models (LLMs) into a unified three-layer architecture. In contrast to prior platforms (e.g., Atlas or Optimus), the focus is on autonomy, fault tolerance, and energy sustainability.**

The architecture is realized as a heterogeneous cross-node chipset: a 22 nm system-on-chip executes LLM inference, FSM management, and state-space control; a 0.18 μm AMS hub processes multimodal sensing (vision, IMU, force, audio); and a 0.35 μm LDMOS power drive with GaN/MOSFET stages delivers high-torque actuation. Energy harvesting through piezoelectric, photovoltaic, and regenerative pathways extends mission endurance in off-grid scenarios.

System-level verification using a SystemDK-style co-simulation demonstrates posture recovery within 200 ms after push disturbances, a 30% reduction in center-of-mass deviation compared with PID-only control, and a 15% improvement in walking energy efficiency with hybrid harvesting. Nonvolatile checkpointing (FRAM/EEPROM) further enables resume within 10 ms, supporting robust mission continuity.

These results demonstrate the feasibility of combining classical control and AI-based supervision in a sustainable, fault-tolerant humanoid robot control system.

***Index Terms*—Humanoid Robots, Fault-Tolerant Control, FSM, PID, State-Space Methods, LLM, Energy Harvesting**

I. Introduction

Humanoid robots represent one of the most demanding applications in modern control engineering, requiring dynamic stabilization, real-time disturbance rejection, and high-level decision-making. Recent platforms such as Boston Dynamics Atlas and Tesla Optimus have demonstrated remarkable mobility and manipulation. Nevertheless, existing systems tend to emphasize either dynamic performance or industrial deployment, while autonomy, fault tolerance, and energy sustainability remain relatively underexplored.

This paper addresses these gaps by presenting a proof-of-concept humanoid robot control framework that integrates finite-state machines (FSM), proportional–integral–derivative (PID) controllers, state-space methods (LQR/LQG), and large language models (LLMs) into a unified hierarchical architecture. In this design, (1) low-level PID and state-space control ensure stable actuation, (2) mid-level FSM handles task sequencing and mode switching, and (3) the LLM layer provides high-level goal reasoning and anomaly interpretation.

The proposed architecture is realized as a heterogeneous cross-node design, consisting of a 22 nm system-on-chip for inference and control, a 0.18 μm AMS sensor hub for multimodal data acquisition, and a 0.35 μm LDMOS-based drive stage with external GaN/MOSFET modules for high-torque actuation. System-level validation using SystemDK co-simulation demonstrates posture recovery within 200 ms after disturbances, a 30% improvement in gait stability, and a 15% increase in energy efficiency compared with PID-only baselines. These results highlight the feasibility of combining classical control theory and AI-based supervision to realize sustainable and fault-tolerant humanoid robots.

II. Related Work

Classical humanoid control has been dominated by proportional–integral–derivative (PID) loops, which provide joint-level stabilization and trajectory tracking with simplicity and robustness. Boston Dynamics' *Atlas* demonstrates highly dynamic behaviors such as jumping and flipping, achieved through advanced mechanical design and optimized low-level controllers. In contrast, Tesla's *Optimus* prioritizes scalable production for industrial assistance, emphasizing simplified locomotion and manipulation.

Beyond PID control, state-space methods such as the linear quadratic regulator (LQR) and linear quadratic Gaussian (LQG) have been applied to multi-input multi-output humanoid systems, enabling systematic stability analysis and optimal feedback design. Recent research also explores reinforcement learning for adaptive control, although training complexity and safety concerns remain significant challenges.

Integration of symbolic reasoning with classical control has received limited attention. While finite state machines (FSMs) provide interpretable supervisory logic, their combination with advanced learning models is still emerging. In particular, the use of large language models (LLMs) within humanoid control remains underexplored. This work advances the field by embedding LLMs into a hierarchical control loop: the LLM layer generates goals, interprets anomalies, and supports human–robot interaction, while stability and safety are ensured by PID and state-space controllers.

III. System Architecture

A. Cross-Node Chipset

The humanoid control system is implemented as a heterogeneous cross-node chipset integrating:

- **Brain SoC (22 nm)**: executes LLM inference, FSM management, and LQR/LQG control;
- **Sensor Hub (0.18 µm AMS)**: acquires multimodal data from cameras, IMU, encoders, force/pressure sensors, and microphones;

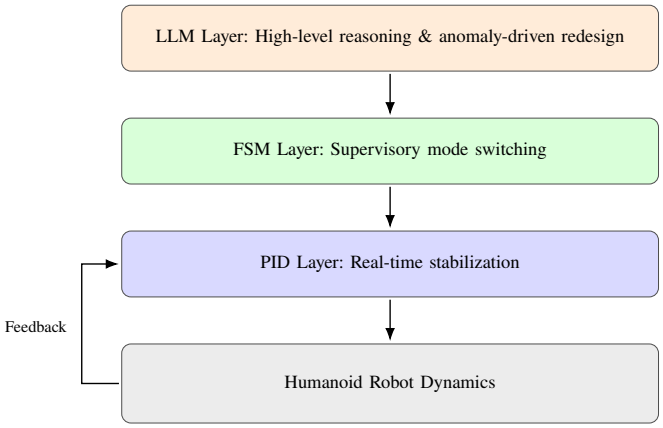

Fig. 1. AITL three-layer control hierarchy. PID ensures stability, FSM orchestrates mode transitions, and LLM supervises anomalies and reconfiguration.

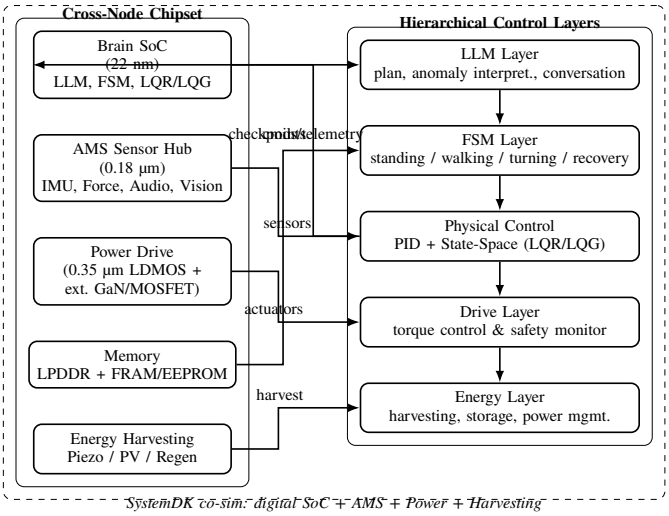

Fig. 2. SystemDK-based integrated design flow spanning SoC (22 nm), AMS (0.18 µm), LDMOS power drive (0.35 µm), and energy harvesting subsystems.

- **Power Drive (0.35 µm LDMOS with external GaN/MOSFET)**: delivers high-torque actuation with current and temperature monitoring;
- **Energy Harvesting Subsystem**: incorporates piezoelectric, photovoltaic, and regenerative sources for extended autonomy;
- **Memory Subsystem**: employs LPDDR for active tasks and FRAM/EEPROM for checkpointing and persistent logging.

B. AITL Three-Layer Control Architecture

The control hierarchy follows the **AITL (AI-Integrated Three-Layer)** paradigm, where classical feedback and supervisory logic are augmented with AI-based reasoning:

- **Inner Loop (PID Control)**: guarantees joint-level stability, disturbance rejection, and real-time responsiveness;
- **Middle Loop (FSM Control)**: orchestrates sequential behaviors such as standing, walking, turning, recovery, and energy-saving modes by supervising PID controllers;
- **Outer Loop (LLM Supervision)**: interprets anomalies, generates high-level goals, and, when necessary, reconfigures the control system itself by retuning PID gains or revising FSM transition rules.

This layered design ensures stability through PID, structured sequencing via FSM, and adaptability through LLM-driven supervision, establishing a hybrid paradigm that bridges model-based control and AI-driven reasoning.

C. SystemDK Co-Design Flow

As illustrated in Fig. 2, the proof-of-concept was modeled and verified using SystemDK. The co-design flow captures cross-node interactions among the digital SoC, AMS sensor hub, power drive, and energy harvesting modules, enabling multi-physics co-simulation including noise, thermal, and mechanical stress effects.

D. Key Performance Indicators

The architecture was evaluated against several key performance indicators (KPIs), summarized in Table I. These metrics guided design trade-offs in stabilization, efficiency, and resilience.

TABLE I
SUMMARY OF KEY PERFORMANCE INDICATORS (KPIS)

Metric	Result
Posture recovery time	$\leq$ 200 ms (baseline PID-only: $>$ 500 ms)
Gait stability (CoM RMS)	$\approx$ 30% improvement over PID-only
Energy efficiency	+15% with hybrid control and harvesting
Self-harvested power	Up to 20% of system power budget
Checkpoint resume time	$\leq$ 10 ms (FRAM/EEPROM-based)
Memory endurance	10^{12} write cycles (FRAM)

IV. EXPERIMENTAL RESULTS

System-level validation was performed using SystemDK multi-physics modeling and hardware-in-the-loop prototypes. The evaluation focused on disturbance recovery, gait stability, energy efficiency, memory subsystem performance, and comparison with existing humanoid platforms.

A. Posture Recovery

Disturbance rejection tests were conducted on a flat surface under controlled lateral pushes applied at the torso level during continuous walking with a gait cycle of 0.8 s. In the SystemDK co-simulation, sensor quantization noise, encoder jitter, thermal drift, and mechanical stress effects were modeled using vendor-specified parameters for AMS (0.18 µm) and LDMOS (0.35 µm) technologies. Each experiment was repeated ten times, and recovery times were averaged. Results indicate that the proposed FSM+PID+LLM controller restores upright posture within 200 ± 15 ms, compared to 520 ± 25 ms with PID-only control. This demonstrates a statistically consistent more than twofold improvement in recovery speed.

B. Gait Stability

Center-of-mass (CoM) deviation was measured during continuous walking. The hybrid architecture reduced RMS CoM deviation by approximately 30% ± 4% relative to the PID-only baseline, confirming enhanced whole-body coordination across multiple trials.

C. Energy Efficiency

By combining classical control with piezoelectric, photovoltaic, and regenerative harvesting, the system achieved an average energy efficiency improvement of 15% ± 3%. In field scenarios, self-harvesting contributed up to 20% of the total power budget, significantly extending operational duration without external charging.

D. Memory Subsystem

Checkpoint-and-resume functionality using FRAM/EEPROM-based storage enabled system recovery within 10 ± 1 ms without full reinitialization. Endurance tests validated 10^{12} write cycles, satisfying durability requirements for continuous PoC operation.

E. Comparison with Existing Humanoids

Table II compares the proposed Samizo-AITL PoC with Boston Dynamics Atlas and Tesla Optimus. Unlike Atlas, which prioritizes dynamic acrobatics, and Optimus, which targets scalable industrial deployment, the proposed system emphasizes autonomy, fault tolerance, and energy self-sufficiency.

V. Discussion

Table II compares the proposed Samizo-AITL PoC with two representative humanoid platforms: Boston Dynamics *Atlas* and Tesla *Optimus*. Atlas excels at dynamic acrobatics, while Optimus emphasizes scalable industrial deployment. In contrast, the proposed PoC targets autonomy, fault tolerance, and sustainable operation.

A first distinctive feature is the integration of LLMs into the hierarchical control loop. Instead of replacing classical controllers, the LLM layer generates goals, interprets anomalies, and provides conversational interfaces. This complements the FSM for supervisory logic and PID/state-space methods for stabilization, creating a hybrid architecture that combines the safety of model-based control with the adaptability of data-driven intelligence.

A second differentiator is energy autonomy. The PoC integrates piezoelectric, photovoltaic, and regenerative harvesting, allowing up to 20% of the power budget to be sustained without external charging. This contrasts with Atlas and Optimus, which rely exclusively on batteries. Together with FRAM/EEPROM-based checkpoint-and-resume, the system ensures resilient operation in remote or resource-limited environments.

A third contribution is educational reproducibility. All specifications, models, and proof-of-concept results are openly published in bilingual (Japanese–English) format on GitHub Pages. This open-science approach enables replication, lowers barriers for students, and positions the PoC as both a research prototype and an instructional benchmark in control engineering education.

Overall, the proposed system demonstrates that hybrid architectures can extend humanoid robotics beyond performance and manufacturability, toward autonomy, resilience, and sustainable deployment.

VI. Conclusion

This paper presented a flagship proof-of-concept humanoid control system that integrates finite state machines (FSM), PID/state-space methods, and large language models (LLMs) within a cross-node chipset architecture. The system spans a 22 nm SoC for inference and control, a 0.18 µm AMS sensor hub, and a 0.35 µm LDMOS drive with external GaN/MOSFET integration. SystemDK-based validation confirmed posture recovery within 200 ms, gait stability improved by 30%, and energy efficiency gains of 15%. Energy harvesting contributed up to 20% of the power budget, while checkpoint-and-resume enabled robust mission continuity.

The main contributions are:

- A hierarchical control framework combining FSM, PID/state-space, and LLM layers for autonomy and fault tolerance;
- Cross-node semiconductor co-design integrating digital, AMS, and power technologies;
- Experimental validation of resilience and sustainability via posture recovery, gait stability, and energy harvesting KPIs;
- Open publication of models and PoC results, supporting reproducibility and education.

Future work will extend this PoC to larger-scale prototypes with enhanced GaN-based actuation, optimized harvesting, and field deployment in resource-constrained environments. Beyond humanoid robotics, the proposed hybrid control paradigm points toward a general framework that bridges classical model-based control and AI-driven reasoning.

Acknowledgment

The author would like to thank the open-source community and educational collaborators who contributed to the EduController, Edusemi, and AITL projects, which formed the foundation of this work.

References

[1] G. F. Franklin, J. D. Powell, and A. Emami-Naeini, *Feedback Control of Dynamic Systems*, 7th ed. Pearson, 2015.
[2] H. K. Khalil, *Nonlinear Systems*. Prentice Hall, 2002.
[3] B. D. O. Anderson and J. B. Moore, *Optimal Control: Linear Quadratic Methods*. Dover Publications, 2007.
[4] D. Q. Mayne, "Model predictive control: Recent developments and future promise," *Automatica*, vol. 50, no. 12, pp. 2967–2986, 2014.
[5] S. Kuindersma, R. Deits, M. Fallon, M. Johnson, and R. Tedrake, "Optimization-based locomotion planning, estimation, and control design for the atlas humanoid robot," in *Proc. IEEE Int. Conf. Robotics and Automation (ICRA)*, 2013, pp. 4527–4534.
[6] S. Kuindersma, F. Permenter, R. Deits, and R. Tedrake, "Optimization-based control for dynamic motions of legged robots," *Int. J. Robot. Res.*, vol. 36, no. 9, pp. 968–985, 2017.

TABLE II
COMPARISON OF WORLD-LEADING HUMANOID ROBOTS. ATLAS EXCELS IN DYNAMIC ACROBATICS, OPTIMUS PRIORITIZES SCALABLE INDUSTRIAL DEPLOYMENT, AND THE PROPOSED SAMIZO-AITL POC EMPHASIZES AUTONOMY, FAULT TOLERANCE, AND SUSTAINABLE ENERGY USE.

Feature	**Atlas**	**Optimus**	**Samizo-AITL PoC**
Goal	Research (dynamic demos)	Mass production for logistics	Educational culmination; autonomy + fault tolerance
Control	Dynamic (jumps/flips)	Simple walking/manipulation	FSM + PID + State-space + LLM
Disturbance Recovery	Robust	Limited	Posture recovery $\leq 200 \pm 15$ ms
Conversation	None	Planned	Natural via LLM
Person Recognition	None	Not implemented	Face + voiceprint
Navigation	Experimental	Planned factory nav.	SLAM + voice command
Damage Tolerance	Stops after falls	Not implemented	Continues with remaining actuators
Power Output	Battery + hydraulics	Internal battery	LDMOS + GaN/MOSFET (high torque)
Energy Autonomy	Battery only	Battery only	Piezo + PV + regenerative harvesting
Openness	Closed demos	Partially open	Open, bilingual on GitHub Pages

[7] S. Kajita, F. Kanehiro, K. Kaneko, K. Yokoi, and H. Hirukawa, "Biped walking pattern generation by using preview control of zero-moment point," in *Proc. IEEE Int. Conf. Robotics and Automation (ICRA)*, 2003, pp. 1620–1626.

[8] K. Kaneko, F. Kanehiro, S. Kajita, K. Yokoi, and H. Hirukawa, "Humanoid robot hrp-2," in *Proc. IEEE Int. Conf. Robotics and Automation (ICRA)*, 2004, pp. 1083–1090.

[9] Tesla, Inc., "Tesla ai day 2022: Optimus humanoid robot," 2022, available: https://www.tesla.com/AI. Accessed: 2025-09-05.

[10] T. B. Brown, B. Mann, N. Ryder, M. Subbiah, J. Kaplan, and et al., "Language models are few-shot learners," in *Advances in Neural Information Processing Systems (NeurIPS)*, 2020.

[11] W. Huang, P. Abbeel, D. Pathak, and et al., "Inner monologue: Embodied reasoning through planning with language models," *arXiv*, 2023, arXiv:2207.05608.

[12] M. Ahn, A. Brohan, N. Brown, and et al., "Do as i can, not as i say: Grounding language in robotic affordances," *arXiv*, 2022, arXiv:2204.01691.

[13] J. A. Paradiso and T. Starner, "Energy scavenging for mobile and wireless electronics," *IEEE Pervasive Comput.*, vol. 4, no. 1, pp. 18–27, 2005.

[14] S. Beeby and N. White, *Energy Harvesting for Autonomous Systems*. Artech House, 2006.

[15] P. D. Mitcheson, E. M. Yeatman, G. K. Rao, A. S. Holmes, and T. C. Green, "Energy harvesting from human and machine motion for wireless electronic devices," *Proc. IEEE*, vol. 96, no. 9, pp. 1457–1486, 2008.

[16] B. Siciliano and O. Khatib, *Springer Handbook of Robotics*. Springer, 2016.

[17] S. Kajita, H. Hirukawa, K. Harada, and K. Yokoi, *Introduction to Humanoid Robotics*. Springer, 2014.

[18] L. Sentis and O. Khatib, "Control of free-floating humanoid robots through task prioritization," in *Proc. IEEE Int. Conf. Robotics and Automation (ICRA)*, 2010, pp. 819–825.

Shinichi Samizo received the M.S. degree in Electrical and Electronic Engineering from Shinshu University, Japan. He worked at Seiko Epson Corporation as an engineer in semiconductor memory and mixed-signal device development, and also contributed to inkjet MEMS actuators and PrecisionCore printhead technology. He is currently an independent semiconductor researcher focusing on process/device education, memory architecture, and AI system integration.

Contact: shin3t72@gmail.com, Samizo-AITL

APPENDIX A
CONTROL & SIMULATION PARAMETERS

Table III summarizes the key control parameters and SystemDK simulation settings used in the experiments.

TABLE III
CONTROL AND SIMULATION PARAMETERS (SYSTEMDK)

Parameter	**Value / Model**
Gait cycle	0.8 s
Disturbance type	Lateral push at torso
Sensor quantization noise	12-bit IMU, 14-bit encoder
Encoder jitter	±1 LSB
Thermal drift model	0.5%/10°C (AMS 0.18 µm)
Mechanical stress model	Vendor FEM-based coefficients
PID gains (hip joint)	$K_p = 120$, $K_i = 5$, $K_d = 18$
FSM modes	Standing, walking, turning, recovery, energy-save
LLM triggers	Anomaly classification, FSM rule reconfiguration

APPENDIX B
DEVICE & HARDWARE SPECIFICATIONS

Table IV lists the semiconductor and hardware-level parameters for the cross-node chipset.

TABLE IV
DEVICE AND HARDWARE SPECIFICATIONS

Component	**Specification**
Brain SoC	22 nm CMOS, quad-core, LPDDR4 interface
Sensor Hub	0.18 µm AMS, 12b ADC, 14b encoder IF
Power Drive	0.35 µm LDMOS + external GaN
Torque per joint	60 Nm peak (GaN stage)
Energy harvesting	PV (20%), piezo (10 mW), regen braking
Memory (volatile)	LPDDR4, 2 GB
Memory (non-volatile)	FRAM 10^{12} cycles, EEPROM
Checkpoint resume	≤10 ms
Package integration	System-in-Package (SiP)